

ELASTIC, INELASTIC AND TIME CONSTANT MEASUREMENT FOR M102 (AL-C-O) DISPERSIONS-REINFORCED ALUMINUM ALLOYS

Purpose. To conduct an experimental study on M102 aluminum alloy bulk content characterization under cyclic loadings for precision applications such as balance machines, optical, and laser instruments. M102 (AL-C-O) dispersion-reinforced aluminum alloy was chosen because of its ability to withstand temperatures beyond 200 °C and has a better strength than precipitation-hardened Al alloys at room temperature. A CNC milling machine is used to manufacture test samples with longitudinal machining directions. A constant time interval is set for the fabric – a quarter-hour span, which is based on the investigation of inelastic and plastic deformations in the nanoscale.

Methodology. An electromagnetic test instrument applies a tensile stress range of 10 to 145 N/mm² to samples with particular shape. It should be noted that interferometers and capacitive sensors were used to measure all forms of deformations with and without loading. The experiments are carried out in a temperature-stable environment of 30.5 °C; measurements are taken within a residual strain range of 10 microns.

Findings. The results obtained show that results for inelastic deformations for samples of longitudinal cuts direction at 30.5 °C were measured under 150 N/mm² stress as 500 nm inelastic deformation and 100 nm plastic deformation were measured, which is much higher than aluminum alloy studied before at room temperature (20 °C). Furthermore, it was found that the time constant of the M102 (AL-C-O) aluminum alloy samples was double times higher than that for other samples,

Originality. For the first time, a study has been conducted on inelastic and plastic deformations in the nanoscale for characterization of M102 aluminum alloy bulk content under cyclic loadings for precision applications.

Practical value. One of the main factors affecting the using of other materials than steel in precision applications such as balance machines, optical, and laser instruments is measurement and determination of inelastic, plastic and time constant of the process of delamination of materials of different aluminum alloys since they are nonmagnetic, are easily machined and shaped. This will bring new products and opportunities for these materials.

Keywords: *M102 (AL-C-O) aluminum alloy, inelastic deformation, plastic deformation, time constant, cyclic loadings*

Introduction. The use of simple test equipment previously designed and built for investigating and measuring plastic deformation, inelastic deformation, and time constant for monolithic spring joints under cyclic loadings is provided throughout this study. Aluminum is appealing for a variety of applications due to its low density. Traditional aluminum materials, on the other hand, are not well suited to high-temperature applications (e.g., engine and turbine construction) since their strength drops dramatically as temperature rises. The continuous range of usage for precipitation-hardened Al alloys is limited to a maximum of 200 °C [1–3].

The lightweight, high strength-to-weight ratio, high temperature strengths, aging effects on tensile strength and toughness, and creep make dispersion-strengthened aluminum alloys and composites particularly appealing. Particulate or whisker reinforcement improves their ability to withstand high temperatures. By integrating SiC particulate into a rapidly solidified, high-temperature AL-C-O (alloy M102) matrix, high-temperature discontinuously reinforced M102 aluminum composites for elevated-temperature applications were produced. To temperatures reaching 500 °C, this composite is comparable with Ti-6Al-4V and steel monoblocks in terms of specific stiffness [3, 4].

To improve heat resistance, procedures for producing dispersion-hardened Al-based materials have been devised, which involve physically alloying ceramic particles in a powder mill and then extruding them at temperatures up to 500 °C. Dispersoids such as oxides and carbides are employed. The particles are 50 nm in size [5, 6].

M102 (AL-C-O) dispersion-reinforced aluminum alloys were chosen because they are suitable for temperatures beyond 200 °C as well as have better strength at room temperature than precipitation-hardened Al alloys. This material's creep resistance is also stated to have been improved [4].

Longitudinal machining directions are used to prepare test samples. Fabric Nano stability is critical for ultra-precision applications including high-frequency inertial and weight-

balancing measurement devices, high rotation speeds laser operation and optical equipment, and small-scale machines. Micro-electro mechanical systems (MEMS Semiconductor, LCD, Solar panel production equipment, Robots, Medical equipment, OA equipment, various molds and tools make another sophisticated application that is concerned with material micro stability since it influences not only the accuracy but also durability of this systems [7–9].

Nano stability, on the other hand, is required for short-term loadings (impulses, shocks, and vibrations) as well as medium- to-long-term loadings without load relaxation of internal stress or imbalance required critical stability requirements and was infected by temperature increases [10–12].

The purpose of the project is to concentrate on inertial applications, specifically precise weighing scales. Steel monoblocks, which are considered mechanical elements, make up most of the components of such scales. An electromagnetic coil is used to apply cyclic loadings to the samples and transfer the block deformation to the output measurement equipment. After the load is discharged, block samples should quickly revert to their original dimensions in each cycle [1]. It is worth noting that the time constant of examined samples, which is the amount of time it takes to complete the process, should be very low [13–15].

These are the disadvantages of the steel monoblocks utilized in this weighing scale, which are being evaluated in this research. As a result, the load measurement method necessitates ultra-precision while weighing at a high frequency and maintaining a high level of stability. As a result, substituting other materials for these elements to confirm the above-mentioned properties should be explored for such scales. Many common materials, such as chromium and nitrogen-containing steels (carbon steels), maraging (non-carbon) steels, bronze (mainly beryllium-containing alloys), and titanium, are now used for stability purposes. To achieve the desired strength, these materials are solution treated, quenched, and aged. Steels, on the other hand, have a higher magnetic permeability than aluminum alloys, which are cheaper, easier to manufactured, with lower

modulus of elasticity value which will increase flexure thickness [16–18].

Another goal of this project was to compare the mechanical properties of different M102 (AL–C–O) dispersion-reinforced aluminum alloys to conventional steel monoblocks and diverse aluminum alloys we examined in prior research work in high-frequency weight measuring devices [1, 2, 19]. In high-frequency weight measurement systems, the indicated alloys were evaluated as a replacement for standard steel monoblocks. The testing load (pulling forces) range was adjusted to 0.2 to 200 N with a programmable factor of 1.1 to 1.4 at a quarter-hour constant time through the electromagnet unit for sample deformation.

Two interferometers and two capacitive sensors are put in various spots on the sample to measure deformation with and without loading. The general testing machine runs in an isothermal environment with a temperature-stable housing, and the measured characteristics include plastic, elastic, and inelastic deformation.

Experimental Setup and Specimen design. 40 mm width, 200 mm length, and 20 mm thickness samples were made of M102 (AL–C–O) dispersion-reinforced aluminum alloys. 2 thin flexures (mid-cross-section $[0.1 \times 20 \text{ mm}^2]$) that can carry variable tension and compression loads were manufactured utilizing a precision milling machine with diamond cutting tools to detect the specimen slight deformation.

The specimen was clamped in a three-point stress-free clamping system within the miller. Early deformation is avoided by free cutting the flexures at the start of the test, which keeps residual stresses produced during the machining process close to the surfaces. The specimen was heat-treated, and the securing portions were loosened just before the test began. Fig. 1 depicts the specimen geometry and illustrates the cutting directions as longitudinal or orthogonal.

Deformation measurement. Two capacitive sensors and two interferometers were used to measure the deformation of the object with ultra-high precision. The capacitive sensors are glued to one side of the specimen in various loca-

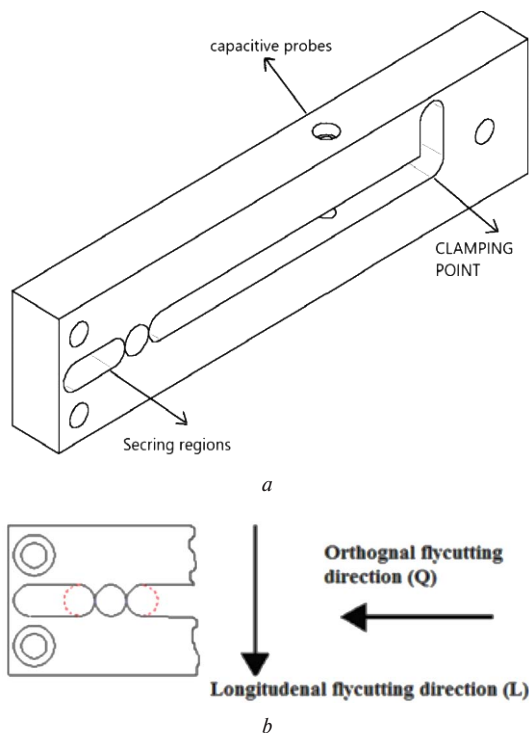


Fig. 1. Tested workpiece and cutting directions (a). An illustration of the geometry of the workpiece (b). Designation applies to longitudinal and orthogonal cuttings [1, 2]

tions. In addition, the interferometers are all on the same surface. Small steel foils were employed to achieve a magnetic connection with retro-reflectors, it should be noted. In addition, the applying force hook was attached, and the interferometer was thus initialized by adjusting the retro, which may freely move on the surface and is only held in place magnetically.

Test machine. The test machine is used to regulate the loading time, which can range from a fraction of a second to several hours.

The test setup machine is made up of aluminum frame with a length of one meter and 4 elephant foot legs that connects the specimen with a quadratic opening to the clamping frame, as well as two cylindrical bearings that connect the interferometer and a force transmission wire. The voice-coil is held in place by the upper plate, which may be clamped to adjust the devices. Ferro-fluid within the air gap enhances the connection of the voice-coil and the magnet for insulation. Furthermore, great attention is paid to prevent thermal deformations of the voice-coil and magnetic assembly from transferring to the specimen during measurement. A force transducer, capacitive sensors, and electronic gadgets are among the other components (not shown within the figure). Fig. 2 depicts a schematic test machine.

Experimental procedures. The experimental machine is completely isolated from the surrounding environment to undertake ultra-precision measurements. The specimen was clamped within the clamping frame to begin the experiment. The data was collected by interferometer, with capacitive sensors, interferometer resolution of 10 nm, capacitive sensor

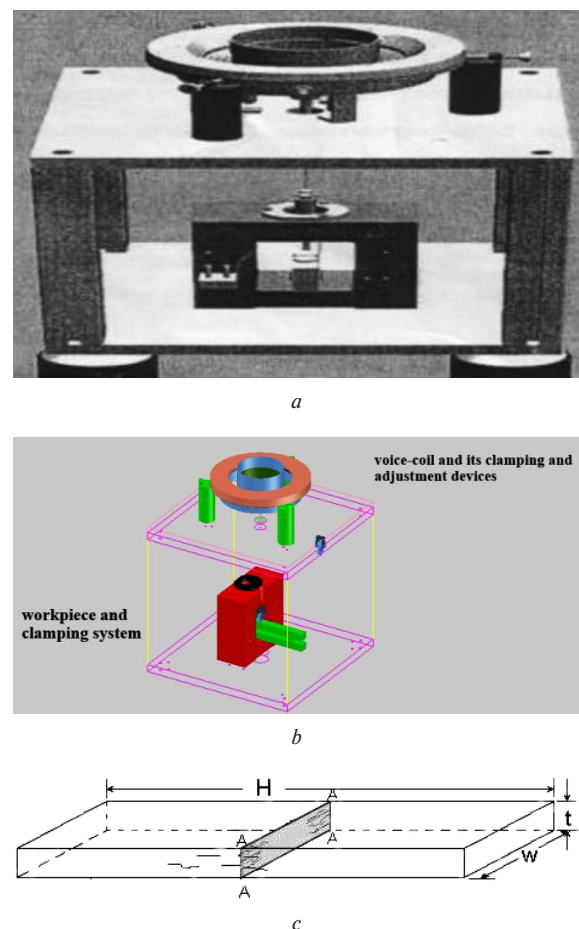


Fig. 2. Test machines and workpiece fixing mechanisms (a). A drawing of the assembly of test machine place gathering accommodate (b), drawing of the assembly of test machine main parts. (c) drawing of workpiece fixing position on test machine [1]

resolution of 0.3 nm, temperature resolution of 0.001 K, measurement, and control of out of doors temperature of 1.0 K, and out of doors vertical vibration of 100 nm suppressed by isolators to 10 nm and digital data filtering to below 1 nm are among the experimental conditions. Moreover, a test cycle typically lasts a few minutes to allow for the storage of capacitive and interferometer data in order to correct for residual temperature effects. After that, cyclic loads with delays are used to isolate the elastic recovery from the plastic strain after unloading. In the next cycle, the loading force is increased by a programmed factor, typically 1.1 to 1.4.

Results and discussion. This paper includes experimental testing and analysis into the feasibility of using M102 (AL–C–O) dispersion-reinforced aluminum alloys, which are primarily suitable for high-temperature applications, in precision monolithic spring joint systems. The pulling force acting on the test samples was created using an electromagnet. An interferometer and a capacitive sensor are used to measure the deformations caused by the force in question. In a temperature-stable housing with an integrated measurement unit, inelastic and plastic deformations are explored with a tensile stress range of 10–160 MPa. The measurement is down to a residual stress of less than 10^{-6} . Experimental measurements are listed in Table.

Plastic and inelastic strain/stress. As temperature has high influence on measured properties of tested samples, it is essential to be sure that it did not change during test.

Fig. 3 shows workpiece temperature measurement. It is clear that during the test time (80 000 Second) difference in temperature is less than 0.5 degree, which is perfect, and gives good indication about the insulation method we used.

When a solid material is subjected to an external force larger than the internal atomic structure force, plastic deformation occurs, and the material is deformed to an irreversible permanent state upon force removal. It is worth noting that this type of distortion is significantly less than that seen in the inelastic scenario.

Fig. 4 depicts the relationship between plastic deformation and tensile stress applied to a specific specimen manufactured from M102 (AL–C–O) dispersion-reinforced aluminum alloys longitudinally machined in a range of stress 10–150 N/mm². It should be noted that identical materials were utilized throughout the current experimental setup, which assessed plastic strain twice using both interferometer and capacitive sensors (KS). Plastic deformation findings acquired by measurement methods described earlier for fiber longitudinal machining directions starting at a stress value of 80 N/mm² when plastic deformation is exactly proportional to tensile stress are clearly seen to follow the same trend. As a result, each sample experiences maximum plastic strain at a tensile stress of 150 N/mm², which is still quite

Table

Inelastic, plastic deformation and time constant for different applied stress for the M102 (AL–C–O) dispersions-reinforced aluminum alloys workpiece

Stress (N/mm ²)	Inelastic deformation interferometer (nm)	Inelastic deformation capacitive sensor (nm)	Plastic deformation interferometer (nm)	Plastic deformation capacitive sensor (nm)	Time constance interferometer (s)	Time constance capacitive sensor (s)
9.84	0.02673	0.0259	1.04347	2.3478	3.67164	2.2280
16.33	0.04321	0.0443	1.08695	1.9565	4.62325	4.9204
33.95	0.09126	0.0977	7.30434	4.3043	4.79771	4.967
70.23	0.21521	0.2218	11.8695	15.173	4.71428	5.717
140.3	0.49291	0.4946	91	100.13	5.29148	6.624

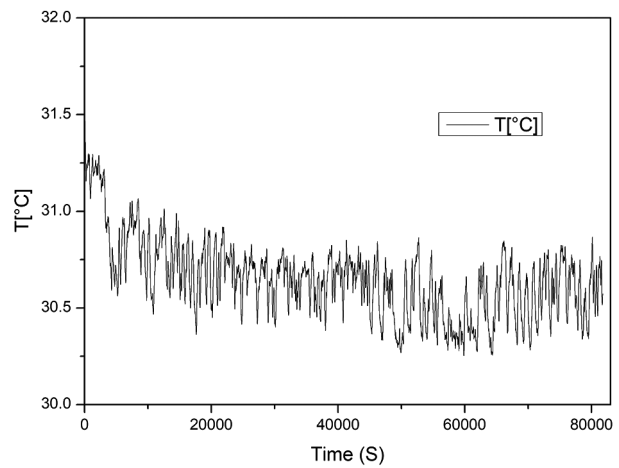


Fig. 3. Workpiece temperature during the test

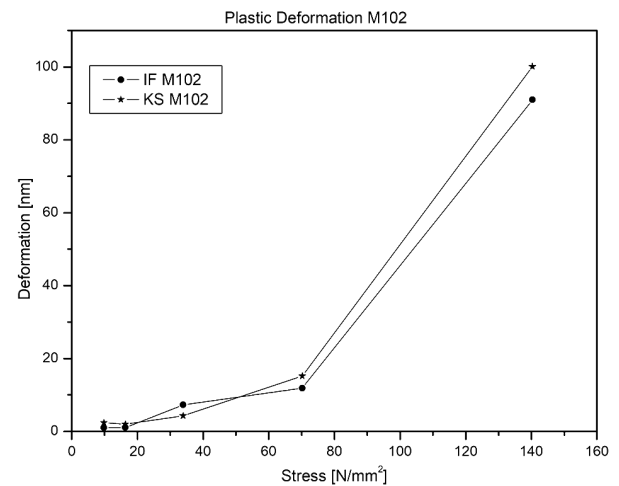


Fig. 4. Plastic deformation M102 with longitudinal cutting direction

minimal when compared to inelastic deformation. For measurements using interferometer (IF) and capacitive sensors (KS), maximum values of plastic deformation are recorded as 100 and 90 nm, respectively. This indicates that distortion under consideration for the M102 (AL–C–O) material is around 90 times greater than 2024 aluminum samples examined in prior research [2].

Furthermore, both interferometer (IF) and capacitive sensors performed well at a stress of 145 N/mm² for an orthogonally machined enclosure (KS). With minor differences, measurement endures essentially the same plastic distortion. The material utilized has a tensile strength of 700 N/mm² and a yield strength of 450 N/mm² at room temperature. The variance is very high, and the results of the interferometer and white capacitive sensors in a wide measuring range change when the stress exceeds 100 N/mm². It should be noted that the test satisfied its metrological probability for measuring plastic deformation. This is the result of electronic drift and temperature changes.

When evaluating the spread of the measured locations from about 150 N/mm², it is worth noting that the measurement findings are more than enough at 20 nm apart.

At 80 N/mm², the difference in sample quality is visible again, where the material changes the slop and form of the measured strait line of the measured values. The difference of approx. 70 nm is shown in this diagram.

Previous research on aluminum 2024 L samples was conducted [2]. In comparison to M102, the plastic deformation behavior in the range of up to 40 N/mm² is radically different

(AL–C–O). Plastic deformation, on the other hand, happens at the start of the endeavor against the tensile force, 2024 L for the samples. Due to plastic deformation, the two higher readings (80 and 150 N/mm²) were recorded at lower deformation than the tensile samples. Up to 80 N/mm² for 14 minutes with 15 minutes between each which is particularly noticeable.

Fig. 5 depicts the inelastic deformation of M102 (AL–C–O) dispersion-reinforced aluminum alloys as a function of stress. Under stress values of 10 and 150 MPa, a minimum of 20 nm and a maximum of 500 nm deformation were detected.

Since inelastic deformation occurs because of micro-creep in the material induced by the movement of the atomic layers in the spring joint during the loading process, the measured value of inelastic deformation was found to be small enough. The glides return to their original position after the weight is released.

The strain on the joints and the pollination period over the previous several hours can influence this behavior. When the stress is increased, however, the material atoms spread further apart without breaking, reaching the yield point, resulting in plastic deformation.

Since this is aluminum that is particle-reinforced with silicon carbide. The particles are 50 nm in size and should be evidenced by a slight inelastic deformation of the material.

Unfortunately, this is not the case here. The material is (even with low loads) significantly worse than all other materials. The reason for this is unknown.

The inelastic deformation is worse by a factor of 20 at all load points. This material is certainly not suitable for a dynamically working measuring cell.

A load of 10 N/mm² in the tension joint already shows a deformation of 26 nm. The material seems to have very high flow properties. The properties of M102 (AL–C–O) dispersion-reinforced aluminum alloys shown at the beginning of this chapter cannot be confirmed here. As before with inelastic deformation, the material already shows high plastic deformation even at low loads.

Time constants. For the tested alloy, Fig. 6 shows the readings of inelastic deformation, plastic deformation, and the time constant during the loading-unloading cycle. The determination of time constants immediately following the measurement point in each time period. Because inelastic deformation is an exponential function (1/e), determining the slope of this line with the discharge curve requires intersecting with horizontal lines, in which the inelastic deformation vanishes, and intersecting the line y = first measuring point with

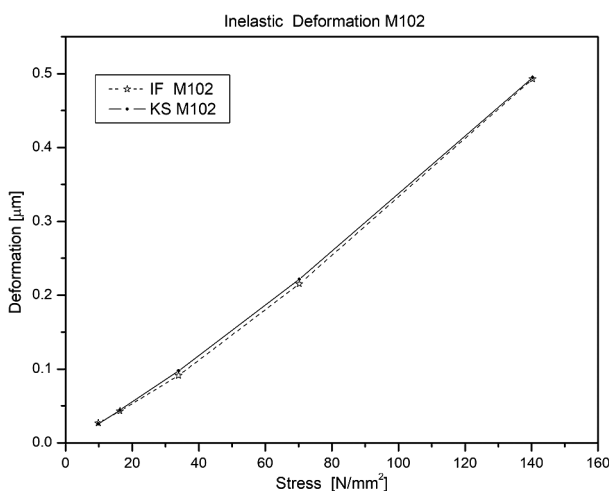


Fig. 5. Inelastic deformation M102 (AL–C–O) dispersion-reinforced aluminum alloys with longitudinal cutting direction

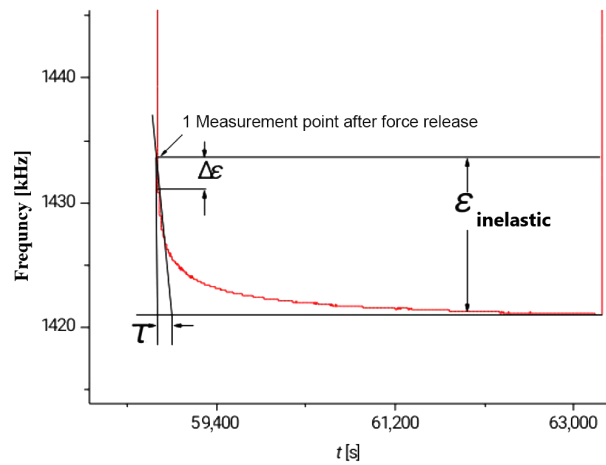


Fig. 6. Determination of the time constant using tangent construction with inelastic deformation

the line x = end defined inelastic deformation produces a period, which is defined as the time constant of the discharge curve.

For straight line it is

$$f(\Delta z) = \frac{0.4 \epsilon_{\text{inelastic}}}{\Delta \epsilon}$$

Similarly, for the same samples machined longitudinally, the influence of tensile stress on time constant is shown in Fig. 7 for a range of 10–150 N/mm². It should be noted that the same measuring devices are utilized in both circumstances. It can be concluded from the figure that time constant values for all samples fluctuate during early stages of stress and until a stress value of 80 N/mm². However, for greater stress values, time constant values remain almost constant, except for KS M102 (AL–C–O), where a considerable rise in time constant values is noticed while increasing stress load to an average time constant value of 6 S, which indicates that that material shows very poor relaxation behavior in the long-term test which is 3 times higher than the previous value of 2024 L aluminum samples tested before. This means the material needs a period of time three times as long until the inelastic deformation is completed.

In the long-term test carried out here, creep effects still occur; according to the manufacturer, the material should have a low creep property. This cannot be confirmed here either.

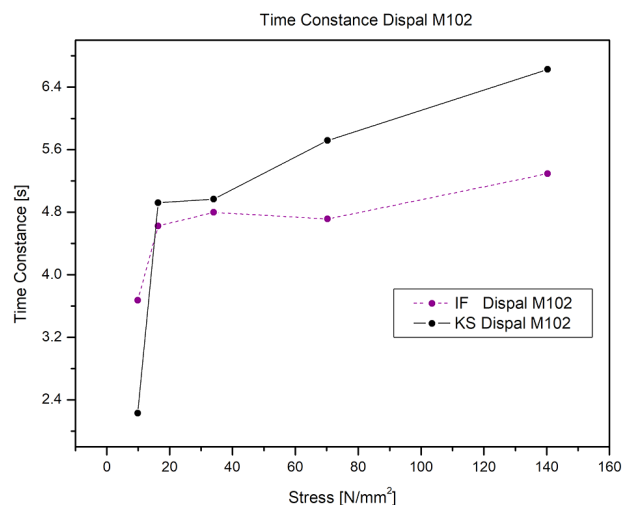


Fig. 7. Time constant of M102 (AL–C–O) dispersion-reinforced aluminum alloys with longitudinal cutting direction

There is a significant variance in time constant values. Since no plastic deformation occurs up to 80 N/mm², the highest load point is a plastic deformation of about 50 % less than in 2024 L. As a result, M102 (AL–C–O) dispersion-reinforced aluminum alloys material clearly falls outside the specified time frame. Even with low loads, the time constant is 2.8 seconds and increases to 6 seconds up to a load of 140 N/mm². The material therefore needs three times the period of time until the inelastic deformation has receded.

Conclusion. Using interferometers and capacitive sensors, this study presents experimental measurements of plastic, inelastic, and time constant of M102 (AL–C–O) dispersion-reinforced aluminum alloy samples machined longitudinally.

Plastic deformation for aluminum alloy samples examined for tensile stress ranges of 10–150 N/mm² is quite minimal.

Plastic deformation for aluminum sample M102 (AL–C–O) is 90 times higher than for 2024 L samples.

Under stress levels of 10 and 150 MPa, measured inelastic deformation ranges from 20 to 500 nm. Furthermore, the results revealed that the sample was significantly greater than the other aluminum alloy types evaluated, which indicates that material has very poor relaxation behavior in the long-term test.

Because electronics are highly sensitive to temperature and humidity, significant variance is seen when detecting plastic, inelastic deformations and calculating time constants for identical samples using interferometers and capacitive sensors.

M102 (AL–C–O) dispersion-reinforced aluminum alloys clearly falls outside the specified time frame. Even with low loads, the time constant is 2.8 seconds and increases to 6 seconds up to a load of 140 N/mm². The material therefore needs three times the period of time until the inelastic deformation has receded.

The M102 (AL–C–O) aluminum alloy samples had a 3 times greater time constant than the other materials.

The nanoscale behavior of materials differs from the micrometer behavior, according to the experimental data. The different alloying elements and percentage of used materials with distinct machining orientations, which in turn created different deformations, could be one reason for the variance in deformation strength.

M102 (AL–C–O) aluminum alloys had worse plastic, inelastic, and temporal constant values when compared to other aluminum types. It is still appealing because it can endure high temperatures, whereas other alloys lose their ductility and ability to tolerate high temperatures.

References.

1. Abushgair, K. (2016). Experimental Evaluation of Material Nano Stability for Ultra Precision Applications, *IOSR-JMCE*, 13(3), 90-97, <https://doi.org/10.9790/1684-1303059097>.
2. Abushgair, K., Al Alawin, A., Alfaqs, F., & Al-Hasan, M. (in press). Experimental Measurement of Material Stability of 2024 T351 Aluminum Alloy for Weight Measurement Applications. *SAE International Journal of Materials and Manufacturing*. <https://doi.org/10.4271/05-15-01-0002>.
3. WolfLuis, W., Aliaga, C. R., Travessa, D. N., Afonso, C. R. M., Bolfarini, C., Kiminami, C. S., & Botta, W. J. (2021). Enhancement of Mechanical Properties of Aluminum and 2124 Aluminum Alloy by the Addition of Quasicrystalline Phases. *Materials Research*, 19(2021), 74-79. <https://doi.org/10.1590/1980-5373-MR-2016-0088>.
4. Shin, S., Park, H., Park, B., Lee, S.-B., Lee, S.-K., Kim, Y., ..., & Jo, I. (2021). Dispersion Mechanism and Mechanical Properties of SiC Reinforcement in Aluminum Matrix Composite through Stir and Die-Casting Processes. *Applied Sciences*, 11, 952. <https://doi.org/10.3390/app11030952>.
5. Mazlan, S., Yidris, N., Koloor, S. S. R., & Petru, M. (2020). Experimental and Numerical Analysis of Fatigue Life of Aluminum Al 2024-T351 at Elevated Temperature. *Metals*, 10, 1581. <https://doi.org/10.3390/met10121581>.
6. Czerwinski, F. (2020). Thermal Stability of Aluminum Alloys. *Materials*, 13(15), 3441. <https://doi.org/10.3390/ma13153441>.

7. Kurek, A., Kurek, M., & Łagoda, T. (2019). Stress-life curve for high and low cycle fatigue. *Journal of Theoretical and Applied Mechanics*, 57, 677-684. <https://doi.org/10.15632/jtam-pl/110126>.
8. Rodeger, H. (2002). Ultra-Precision Flexure Hinge Design and Applications. *EUSPEN: proceedings of the 3rd international conference*, May 26–30, 2002, Eindhoven, the Netherlands. Retrieved from <https://research.tue.nl/en/publications/euspens-proceedings-of-the-3rd-international-conference-may-26-30>.
9. Yang, L., & Ying, L. (2007). A Linear Motor Position Control Based on the Artificial Immune Clustering Methodology. *Chinese Control Conference*, 2007, 6-9. <https://doi.org/10.1109/CHICC.2006.4346870>.
10. Gheisari, R., Ghasemi, A. A., Jafarkarimi, M., & Mohtaram, S. (2014). Experimental studies on the ultra-precision finishing of cylindrical surfaces using magnetorheological finishing process. *Production and Manufacturing Research*, 2(1), 550-557. <https://doi.org/10.1080/21693277.2014.945265>.
11. Ferrara-Bello, A., Vargas-Chable, P., Vera-Dimas, G., Vargas-Bernal, R., & Tecpoyotl-Torres, M. (2021). XYZ Micro positioning System Based on Compliance Mechanisms Fabricated by Additive Manufacturing. *Actuators*, 10, 68. <https://doi.org/10.3390/act10040068>.
12. Choi, S. B., Kim, H. K., Lim, S. C., & Park, Y. P. (2001). Position tracking control of an optical pick-up device using piezoceramic actuator. *Mechatronics*, 11(6), 691-705. [https://doi.org/10.1016/S0957-4158\(00\)00035-0](https://doi.org/10.1016/S0957-4158(00)00035-0).
13. Choi, S. B., & Han, S. S. (2007). A magnification device for precision mechanisms featuring piezoactuators and flexure hinges: Design and experimental validation. *Mechanism and machine theory*, 42, 1184-1198. <https://doi.org/10.1016/j.mechmachtheory.2006.08.009>.
14. Ha, J. L., Kung, Y. S., Hu, S. C., & Fung, R. F. (2006). Optimal design of a micro-positioning Scott–Russell mechanism by Taguchi method. *Sensors and Actuators A: Physical*, 25(2), 565-572. Retrieved from <http://192.83.194.199:8080/handle/987654321/20342>.
15. Van Huis, M. A., Chen, J. H., Zandbergen, H. W., & Sluiter, M. H. F. (2006). Phase stability and structural relations of nanometer-sized, matrix-embedded precipitate phases in Al-Mg-Si alloys in the late stages of evolution. *Acta material*, 54(11), 2945-2955. Retrieved from <http://www.paper.edu.cn/scholar/showpdf/MUz2QNY-IOTA0eQxeQh>.
16. Davis, J. R., Davis & Associates (2013). *Aluminium and Aluminium Alloys. ASM Specialty Handbook*. Ohio. <https://doi.org/10.1361/aut-b2001p351>.
17. Al-Haidary, J., Haddad, J., Alfaqs, F., & Zayadin, F. (2021). Susceptibility of Aluminum Alloy 7075 T6 to Stress Corrosion Cracking. *SAE International Journal of Materials and Manufacturing*, 14(2). <https://doi.org/10.4271/05-14-02-0013>.
18. Craig, W. (2013). *Metals Handbook, Ninth Edition, Heat Treating ASM Handbook*, (Vol. 4). Ohio. Retrieved from https://www.asminternational.org/documents/10192/1849770/5344G_TOC.pdf.
19. *ASM Handbook Committee Metals Handbook Ninth Edition, Properties and Selection: Nonferrous and Pure Metals ASM Handbook*, (Vol. 2). Ohio. Retrieved from <https://app.knovel.com/web/toc.v/cid:kpASMHPV07/viewerType:toc/>.

Вимірювання пружних, пластичних і постійних часу для алюмінієвих армованих сплавів дисперсією M102 (AL–C–O)

Халіл Абушгайр

Кафедра машинобудування, факультет інженерних технологій, Аль-Балка прикладний університет, м. Амман, Йорданія, e-mail: abushgair@bau.edu.jo

Мета. Провести експериментальне дослідження характеристики вмісту сипучих матеріалів з алюмінієвого сплаву M102 при циклічних навантаженнях для точних застосувань, таких як балансирні машини, оптичні й лазерні прилади. Підсилений дисперсіями алюмінієвий сплав M102 (AL–C–O) був обраний через його здатність витримувати температури понад 200 °C і має кращу міцність, ніж дисперсійно-тверді сплави за кімнатної температури. Фрезерний верстат з ЧПУ використовується для виготовлення зразків для випробування з поздовжніми напрямками обробки. Для матеріалу встановлено постійний проміжок часу – чверть години, що заснований на

дослідженні непружних і пластичних деформацій у наномасштабі.

Методика. Електромагнітний прилад для вимірювання застосовує діапазон напружень розтягування від 10 до 145 Н/мм² до зразків з особливою формою. Слід зазначити, що інтерферометри та ємнісні датчики використовувались для вимірювання всіх форм деформацій із навантаженням та без нього. Експерименти проводяться в термостабільному середовищі 30,5 °С, вимірювання проводяться в діапазоні залишкових деформацій 10 мкм.

Результати. Отримані дані показують, що результати непружних деформацій для зразків напрямку поздовжнього зрізу за 30,5 °С вимірювали під напругою 150 Н/мм², оскільки вимірювали непружну деформацію 500 нм та пластичну деформацію 100 нм, що набагато вище, ніж сплав алюмінію, який досліджувався раніше за кімнатної температури (20 °С). Крім того встановлено, що постійна часу для зразків алюмінієвого сплаву М102 (AL–С–О) удвічі перевищує цей показник для інших зразків.

Наукова новизна. Уперше проведене дослідження непружних і пластичних деформацій у наномасштабі для характеристики об'ємного вмісту алюмінієвого сплаву М102 при циклічних навантаженнях для точного застосування.

Практична значимість. Один з основних факторів, що впливає на використання інших матеріалів, крім сталі, у прецизійних додатках, таких як балансирні машини, оптичні й лазерні прилади, це вимірювання й визначення нееластичної, пластичної та постійної часу процесу розшарування матеріалів різних алюмінієвих сплавів, оскільки вони немагнітні, легко піддаються механічній обробці та формуванню. Це принесе нові продукти й можливості для цих матеріалів.

Ключові слова: *алюмінієвий сплав М102 (AL–С–О), непружна деформація, пластична деформація, постійна часу, циклічні навантаження*

Recommended for publication by Dr. Jamil Haddad. The manuscript was submitted 24.02.21.